Mon. Not. R. Astron. Soc. **377,** 1295–1300 (2007) doi:10.1111/j.1365-2966.2007.11689.x

The quasi-persistent neutron star soft X-ray transient 1M 1716−315 in quiescence

P. G. Jonker,[1,2,3★] C. G. Bassa[3] and S. Wachter[4]

[1]*SRON, Netherlands Institute for Space Research, Sorbonnelaan 2, 3584 CA, Utrecht, the Netherlands*
[2]*Harvard-Smithsonian Centre for Astrophysics, 60 Garden Street, Cambridge, MA 02138, USA*
[3]*Astronomical Institute, Utrecht University, PO Box 80000, 3508 TA, Utrecht, the Netherlands*
[4]*Spitzer Science Center, California Institute of Technology, 1200 E. California Blvd., Pasadena CA 91125, USA*

Accepted 2007 March 1. Received 2007 February 28; in original form 2006 August 1

ABSTRACT

We report on our analysis of a 20 ks *Chandra* X-ray observation of the quasi-persistent neutron star soft X-ray transient (SXT) 1M 1716−315 in quiescence. Only one source was detected in the *HEAO-1* error region. Its luminosity is 1.6×10^{32}–1.3×10^{33} erg s^{-1}. In this, the range is dominated by the uncertainty in the source distance. The source spectrum is well described by an absorbed soft spectrum, e.g. a neutron star atmosphere or blackbody model. No optical or near-infrared counterpart is present at the location of the X-ray source, down to a magnitude limit of $I \gtrsim 23.5$ and $K_s \gtrsim 19.5$. The positional evidence, the soft X-ray spectrum together with the optical and near-infrared non-detections provide strong evidence that this source is the quiescent neutron star SXT. The source is 10–100 times too bright in X-rays in order to be explained by stellar coronal X-ray emission. Together with the interstellar extinction measured in outburst and estimates for the source distance, the reported optical and near-infrared limit give an upper limit on the absolute magnitude of the counterpart of $I > 8.6$ and $K_s > 5.1$. This implies that the system is either an ultra-compact X-ray binary having $P_{\rm orb} < 1$ h or the companion star is an M-dwarf. We reconstructed the long-term X-ray light curve of the source. 1M 1716−315 has been active for more than 12 yr before returning to quiescence, the reported *Chandra* observation started 16.9 ± 4.1 yr after the outburst ended.

Key words: accretion: accretion discs – stars: individual: 1M 1716−315 - binaries: general – stars: neutron – X-rays: binaries.

1 INTRODUCTION

Low-mass X-ray binaries (LMXBs) are highly evolved, interacting binaries in which a neutron star or black hole accretes matter via an accretion disc which is fed by a cool, low-mass star (typically $M \lesssim 1\,{\rm M}_\odot$). Some systems have an orbital period of less than ∼1 h (ultra-compact X-ray binaries; UCXBs). These ultra-compact systems are so compact that the donors cannot be main-sequence stars, but instead must be hydrogen-poor (semi) degenerate stars (e.g. Verbunt & van den Heuvel 1995). Belczynski & Taam (2004) predict that about half of the total population of LMXBs may be in UCXBs. A large fraction of the LMXBs are found to be transient systems – the so-called soft X-ray transients (SXTs; e.g. see Chen, Shrader & Livio 1997).

A special group of SXTs has several-year long outbursts before they return to quiescence. These quasi-persistent systems provide an ideal testing ground since the accretion history is well constraint. Furthermore, the idea is that the long outburst has heated the neutron star crust to temperatures higher than that of the neutron star core. Therefore, the (evolution of the) quiescent X-ray luminosity provides information on the cooling properties of the neutron star, which in turn depend on the neutron star equation of state (Brown, Bildsten & Rutledge 1998; Colpi et al. 2001; Wijnands et al. 2001; Rutledge et al. 2002; Cackett et al. 2006a).

1M 1716−315 was first detected in OSO-7 observations obtained between 1971 September 29 and 1974 May 18 (Markert et al. 1975). The last reported detection was by Warwick et al. (1988) using *EXOSAT* observations obtained in 1984 June 14–18. The source was not detected by the *ROSAT* all sky survey (Voges et al. 1999). Large X-ray flares lasting ≈10 min have been reported (Markert, Backman & McClintock 1976). These and other (shorter) flares reported by Jernigan et al. (1978) would now most likely be classified as type I X-ray bursts. The confirmation of the occurrence of type I X-ray bursts and hence of the neutron star nature of the compact object in 1M 1716−315 was given by the detection of three bursts by the *Hakucho* satellite (Makishima et al. 1981). Later *Hakucho* detected a long radius expansion burst (Tawara et al. 1984b). The properties

★E-mail: p.jonker@sron.nl

of this burst were used by Tawara et al. (1984a) to derive a distance of ∼6 kpc (Jonker & Nelemans 2004 derived $d = 5.1$–6.9 kpc using the properties of the same burst; the range depends on whether the burst was hydrogen- or helium-rich).

The source position was determined to 90 arcsec by *SAS-3* (90 per cent confidence; Jernigan et al. 1978). The position was later refined by *HEAO-1* to an area with an equivalent circular radius of 23 arcsec (90 per cent confidence; Reid et al. 1980). The extinction towards the source is low for a LMXB; Christian & Swank (1997) report an equivalent hydrogen column density of $N_{\rm H} = (2.1 \pm 0.6) \times 10^{21}$ cm^{-2}. Wachter, Wellhouse & Bandyopadhyay (2005) observed the source for 1 ks with the High Resolution Camera onboard the *Chandra* satellite but did not detect the source; they report an upper limit on the flux of 2.8×10^{-14} erg cm^{-2} s^{-1}. In this article, we report on a deeper *Chandra* observation of the neutron star SXT 1M 1716−315 in quiescence. We further report on optical Magellan and near-infrared Blanco observations obtained while the source was in quiescence.

2 OBSERVATIONS, ANALYSIS AND RESULTS

2.1 X-ray observations

We observed 1M 1716−315 with the back-illuminated S3 CCD chip of the Advanced CCD Imaging Spectrometer (ACIS) detector onboard the *Chandra* satellite. The observations started on MJD 53567.604 (UTC; 2005 July 16). The net, on-source exposure time was ∼20 ks. The data telemetry mode was set to *very faint* to allow for a better background subtraction. After the data were processed by the *Chandra* X-ray Center (ASCDS version 7.6.0), we analysed them using the CIAO 3.3 software developed by the *Chandra* X-ray Center. We reprocessed the data to clean the background taking full advantage of the *very faint* data mode. We searched the data for background flares but none was found, hence we used all data in our analysis. Using the CIAO tool WAVDETECT, we detect and determine positions of 20 sources in the field of view of the ACIS-S3 CCD (see Fig. 1 and Table 1).

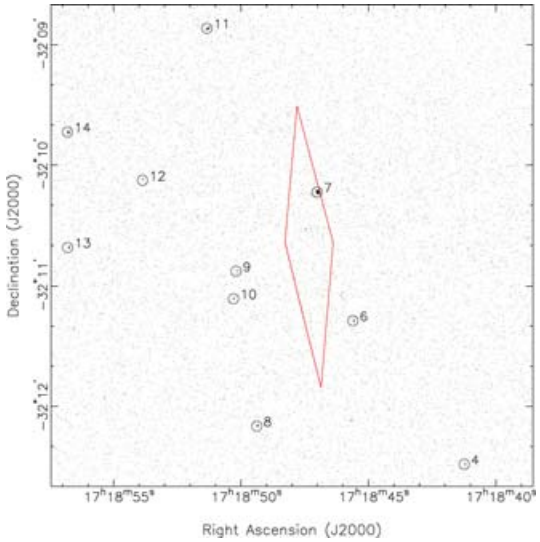

Figure 1. Part (4×4 arcmin^2) of *Chandra*'s ACIS-S3 CCD is shown. The diamond-shaped region is the *HEAO-1* error region of 1M 1716−315. Only one of the detected sources is consistent with that position. The circles indicate the positions of detected X-ray sources (see Table 1 for the numbering).

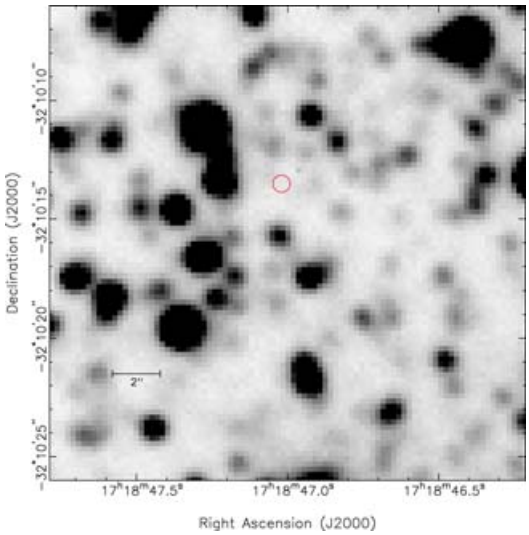

Figure 2. An *I*-band finder chart of the field of 1M 1716−315 obtained with Magellan/IMACS (north is up and east is left). The small circle indicates the position of the *Chandra* detected X-ray Source 7 (radius error circle 0.36 arcsec, 99 per cent confidence).

2.2 Optical observations

In order to search for the optical counterpart in quiescence, we have obtained *I*-band images with the Inamori-Magellan Areal Camera and Spectrograph (IMACS) instrument mounted on the 6.5-m Magellan-Baade Telescope on 2005 July 7, 00:00:35 UTC (MJD 53558.0004 UTC). Exposure times of 10 s and 2×300 s were used. IMACS is a mosaic of eight $4\,{\rm k} \times 2\,{\rm k}$ CCDs that were operated in a 2×2 binning mode. The seeing was 0.7 arcsec. We calibrated all eight CCD chips of the 10 s *I*-band image against stars from the second version of the United States Naval Observatory CCD Astrograph Catalog (UCAC2; Zacharias et al. 2004). Between 13 and 28 stars were used to compute the transformation for each chip, giving typical rms residuals of 0.058 and 0.051 arcsec on α and δ, respectively. From the 20 X-ray sources found on the ACIS-S3 chip, eight coincided with relatively bright stars on the 10 s *I*-band image (see Table 1) having *I*-band magnitudes between 11 and 16. The celestial positions of these stars were measured from the calibrated images and compared with the X-ray positions to determine a boresight correction of $\Delta\alpha = -0.001 \pm 0.037$ arcsec and $\Delta\delta = +0.016 \pm 0.035$ arcsec. Using this boresight correction, we obtained positions and uncertainties for the 20 sources detected by *Chandra* on the S3 CCD chip (see Table 1).

Subsequently, the astrometric solution of the 10-s frame was transferred to the 300-s images using ∼1700 stars. In this, the rms uncertainty was 0.037 arcsec in each coordinate. For the X-ray source in the *HEAO-1* error region, the uncertainty in its location due to the wavelet fitting in WAVDETECT is 0.045 arcsec in α and 0.038 arcsec in δ. Adding all the errors in quadrature gives at the 99 per cent confidence level a radius for the error circle of 0.36 arcsec. The images have been corrected for bias and flat-fielded with IRAF.[1]

2.3 Near-infrared observations

We have also obtained near-IR K_s band data with the Blanco 4-m telescope and Infrared Side Port Imager (ISPI) at Cerro Tololo

[1] IRAF is distributed by the National Optical Astronomy Observatories.

Table 1. Names, coordinates and detection significance of the 20 sources detected by *Chandra* on the S3 CCD chip sorted on right ascension.

Number & name	α (h:m:s $\pm$ arcsec, J2000.0)	δ(°: ′: ″ $\pm$ ″, *J*2000.0)	σ
1 CXOU J171830.7−320927[a]	17:18:30.69 ± 0.18	−32:09:27.31 ± 0.13	11.9
2 CXOU J171833.1−320630[b,a]	17:18:33.10 ± 0.10	−32:06:30.85 ± 0.08	44.2
3 CXOU J171836.0−320940[a]	17:18:36.01 ± 0.13	−32:09:40.40 ± 0.11	17.1
4 CXOU J171841.2−321228	17:18:41.24 ± 0.19	−32:12:28.90 ± 0.19	5.1
5 CXOU J171842.4−320643[a]	17:18:42.40 ± 0.32	−32:06:43.74 ± 0.18	7.1
6 CXOU J171845.6−321117	17:18:45.61 ± 0.12	−32:11:17.32 ± 0.17	7.1
7 CXOU J171847.0−321013[c]	17:18:47.02 ± 0.08	−32:10:13.54 ± 0.07	41.9
8 CXOU J171849.4−321209	17:18:49.38 ± 0.14	−32:12:09.93 ± 0.13	7.8
9 CXOU J171850.2−321053	17:18:50.19 ± 0.16	−32:10:53.03 ± 0.19	4.8
10 CXOU J171850.3−321106	17:18:50.30 ± 0.20	−32:11:06.35 ± 0.22	4.8
11 CXOU J171851.3−320851[b]	17:18:51.34 ± 0.15	−32:08:51.77 ± 0.11	12.3
12 CXOU J171853.9−321007	17:18:53.86 ± 0.23	−32:10:07.64 ± 0.24	4.6
13 CXOU J171856.8−321041[b]	17:18:56.80 ± 0.14	−32:10:41.14 ± 0.14	9.5
14 CXOU J171856.8−320943[b]	17:18:56.81 ± 0.13	−32:09:43.55 ± 0.14	11.2
15 CXOU J171858.0−320932[a]	17:18:58.00 ± 0.27	−32:09:32.44 ± 0.28	4.6
16 CXOU J171859.2−321147[b,a]	17:18:59.22 ± 0.10	−32:11:47.86 ± 0.10	16.1
17 CXOU J171900.2−320958[a]	17:19:00.25 ± 0.23	−32:09:58.98 ± 0.22	5.2
18 CXOU J171903.3−321123[b,a]	17:19:03.30 ± 0.11	−32:11:23.40 ± 0.11	26.8
19 CXOU J171903.4−320925[b,a]	17:19:03.35 ± 0.20	−32:09:25.24 ± 0.21	7.6
20 CXOU J171905.0−321023[b,a]	17:19:04.98 ± 0.11	−32:10:23.14 ± 0.11	21.5

[a]This source is outside the field shown in Fig. 1.
[b]Bright optical star at the X-ray position used for boresight correction.
[c]1M 1716−315 in quiescence.

Inter-American Observatory (CTIO) on 2004 July 25 UTC. The observation consists of three 20-s co-adds at nine dither positions. The data were flat-fielded, sky background subtracted and combined into a single final image in the standard manner using IRAF. ISPI has a pixel scale of 0.3″pixel^{-1} and the seeing conditions during the observations varied between 0.9–1.0 arcsec. We have derived a photometric calibration transformation for the final combined image based on a comparison to Two-Micron All-Sky Survey (2MASS) measurements, neglecting any colour terms since we only have data in one filter. The formal rms error in the transformation fit was 0.04 mag.

2.4 The quiescent X-ray counterpart to 1M 1716−315?

Only one source is detected in the *HEAO-1* error region of 1M 1716−315 (Source 7 in Table 1). Hence, Source 7 is a strong counterpart candidate. In the error circle of Source 7 on the optical *I*-band image there is no object present (see Fig. 2). We estimate a 5σ detection limit of $I > 23.5$ (see Jonker et al. 2006). Furthermore, no K_s counterpart is detected in the *Chandra* error circle and we estimate a detection limit of $K_s > 19.5$. There are three other sources detected in X-rays that have a position close to the error region (Sources 6, 9 and 10 using the numbering from Table 1 in Fig. 1). For none of these sources we detected the *I*- or K_s-band counterpart. In the case of the X-ray Source 9, a bright source was present in both the *I*-band and the K_s-band image at a location close to, but not consistent with, its *Chandra* error circle. The wings of the point spread function of the bright star, however, cover the *Chandra* error circle of Source 9 raising the level of the background considerably. This precludes us from putting firm limits on the presence of a star at the position of the X-ray Source 9. Hence, on the basis of the optical to X-ray luminosity ratio one cannot rule out any of these sources as the potential counterpart of 1M 1716−315. Furthermore, the X-ray source in the error circle could in principle be unrelated to 1M 1716−315: the quiescent X-ray counterpart of 1M 1716−315 could be fainter than our detection limit. In a 1 arcsec circle, placed randomly in the *HEAO-1* error region, we find 0–3 counts. Using the conservative limit of three counts (Gehrels 1986), this converts to a 95 per cent count rate upper limit of 3.9×10^{-4} counts s^{-1}. For a power law with index 2 and an $N_{\rm H} = 2.1 \times 10^{21}$ cm^{-2}, this yields a 3×10^{-15} erg cm^{-2} s^{-1} limit on the 0.5–10 keV flux. For a distance of 6.9 kpc, this gives a limit on the 0.5–10 keV luminosity of 2×10^{31} erg s^{-1}.

2.5 The X-ray spectrum and light curve

We extracted the X-ray photons from a circular region with a diameter of 3 arcsec of Sources 7, 6, 9 and 10. For Source 7, background photons were extracted from an annulus centred on the source with an inner and outer radius of 10 and 40 arcsec, respectively. For Source 7, we detect 185 source photons in the 19 924-s long effective exposure. Hence, the source count rate is $(9.3 \pm 0.7) \times 10^{-3}$ counts s^{-1}. The light curve of the source is consistent with being constant. At these low background-subtracted count rates, photon pile-up is unimportant. We searched for spectral variability during the observation by comparing the mean energy and the variance therein of the photons in the first half of the observation with that of the second half. The two values are consistent with being the same. Even though the shape of the spectrum can have changed keeping the mean energy and its variance constant, it is more likely that within the accuracy of our data the spectrum did not change during the observation. In order to validate the use of the χ^2 fitting technique in the spectral analysis, the source spectrum was rebinned such that each of the spectral bins contained at least 10 counts.

Table 2. Best fit parameters of the quiescent spectrum of 1M 1716−315. NSA stands for neutron star atmosphere and BB refers to blackbody. All quoted errors are at the 68 per cent confidence level. The value in between brackets in the unabsorbed flux column denotes the 95 per cent upper limit to the fractional contribution of a power law (the power law index was fixed at 2; see text).

Model	$N_{\rm H} \times 10^{21}$ cm^{-2}	BB radius $(\frac{\rm d}{10\,\rm kpc})^2$ km	NSA norm. d (kpc)	Temp. BB (keV)/NSA log K/keV$^{\infty}$	Unabs. 0.5–10 keV flux (erg cm^{-2} s^{-1})	Abs. 0.5–10 keV flux (erg cm^{-2} s^{-1})	$\chi^2_{\rm red}$ d.o.f.
BB	2.1[a]	0.4 ± 0.1	–	0.33 ± 0.02	$(5.0^{+0.3}_{-0.8}) \times 10^{-14}$ (19 per cent)	$(3.3^{+0.2}_{-0.4}) \times 10^{-14}$	1.16/13
NSA	2.1[a]	–	53 ± 11	$6.42 \pm 0.04/0.17 \pm 0.02$	$(5.4^{+2.2}_{-2.6}) \times 10^{-14}$ (18 per cent)	$(3.7^{+1.2}_{-1.6}) \times 10^{-14}$	1.39/13
BB	7 ± 2	5^{+9}_{-5}	–	0.24 ± 0.03	$(1.3^{+0.1}_{-0.6}) \times 10^{-13}$ (16 per cent)	$(3.1^{+0.1}_{-1.4}) \times 10^{-14}$	0.64/12
NSA	9 ± 2	–	$3.9^{+b}_{-2.3}$	$6.07 \pm 0.08/0.078 \pm 0.014$	$(2.4^{b}) \times 10^{-13}$ (8 per cent)	$(3.2^{b}) \times 10^{-14}$	0.63/12

[a] Parameter fixed.
[b] Error range is unconstrained.

The 0.3–10 keV X-ray spectrum was fitted with XSPEC 11.3.1 (Arnaud 1996). The fit function consists of an absorbed neutron star atmosphere (NSA; Pavlov, Shibanov & Zavlin 1991; Zavlin, Pavlov & Shibanov 1996), blackbody or power-law model. Each of these absorbed models provides an acceptable fit to the X-ray spectrum in terms of reduced χ^2. However, the best-fitting power-law index was very high with $6.4^{+1.1}_{-0.8}$ and the interstellar extinction was $1.5 \pm 0.3 \times 10^{22}$ cm^{-2} in this case, higher than the best-fitting value found in outburst (errors here and below are at the 68 per cent confidence level). For these reasons, we do not consider the single absorbed power-law model any further. We provide the best-fitting parameters for the blackbody and the NSA model in Table 2 (see also Fig. 3). In order to determine the upper limit on the contribution of a power law to the 0.5–10 keV X-ray flux, we determine the best fit using a model without a power law. Next, we fix all the parameters related to this model and add a power law to the fit function. The power-law index is fixed to the value 2. Hence, the only free parameter is the power-law normalization. After fitting, we determine the 90 per cent confidence error. The outcome of the error in the positive scan direction is added to the value of the power-law normalization. The normalization of the other model components is set to zero as well as the parameter for the interstellar extinction. Subsequently, the flux in only the power-law component is derived. Finally, this flux is expressed as a fraction of the flux in the other model components. We give this 95 per cent confidence upper limit in between brackets in Table 2.

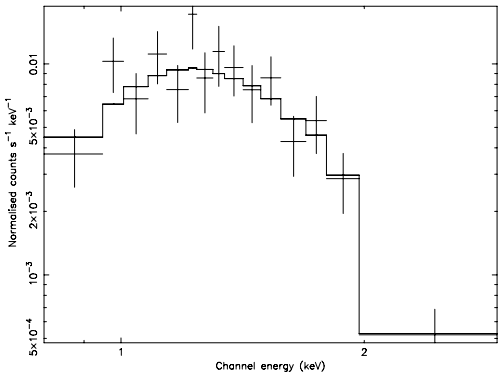

Figure 3. The 0.5–10 keV X-ray spectrum of 1M 1716−315 (Source 7) in quiescence obtained with *Chandra*'s ACIS-S on MJD 53567.604 (UTC; 2005 July 16). The solid line represents the best-fitting absorbed NSA model where $N_{\rm H}$ is a free-floating fit parameter.

For Sources 6, 9 and 10, we only detected 24, 14 and 13 photons in the energy range 0.3–10 keV in the 3 arcsec source area, respectively. Out of these, there are approximately 7 ± 3 background photons. We have tried to model the X-ray spectra in XSPEC 11.3.1 making use of the C-statistics; however, the model parameters are unconstrained. In order to investigate the spectral properties of these sources, keeping in mind that the background photons generally have a hard spectrum, we determine the number of photons in the 0.3–1.5 and 1.5–10 keV energy band and the mean energy in the 0.3–1.5 and 1.5–10 keV bands. For Sources 6, 9, and 10, we find 7/17, 2/12 and 2/11 photons in the 0.3–1.5 keV/1.5–10 keV band, respectively. The mean 0.3–1.5 keV/1.5–10 keV energy and the variance therein for Source 6, 9 and 10 are 1.2 ± 0.3 keV/3.3 ± 2.2 keV, 1.2 ± 0.1 keV/4.6 ± 2.7 keV and 1.0 ± 0.2 keV/4.4 ± 2.4 keV, respectively. One cannot exclude Sources 6, 9 and 10 on the basis of their hard spectra alone as possible quiescent counterparts of the neutron star SXT 1M 1716−315 since some neutron stars have been found to have a hard spectrum at low luminosities in quiescence (see e.g. Jonker et al. 2004). However, only Source 7 has a spectrum that is consistent with a soft spectrum as often found for a quiescent neutron star. Whereas coronal activity from a star might also yield a soft spectrum (for a review see Güdel 2004), we find no evidence in the optical or near-infrared for the presence of such a star. From figure 2 in Güdel (2004), the observational *I*-band limit and the observed X-ray flux, it can be derived that in order to explain the X-ray emission as coronal X-ray emission of a star, that star would need to be several orders of magnitude brighter than has been found before in order to explain the observed X-ray flux and the optical non-detection. This makes the identification of the X-ray source as stellar coronal X-ray emission unlikely. Instead, we conclude that based on the positional coincidence, the spectral properties together with the optical and near-infrared upper limits, it is very likely that Source 7 is the quiescent neutron star counterpart to 1M 1716−315.

With the new accurate *Chandra* X-ray position from our ACIS-S observation in hand, we re-analysed the HRC-I observation of Wachter et al. (2005). Only one photon is detected in the 0.67 arcsec 90 per cent confidence error circle centred on the best-fitting source position (taking into account the nominal 0.6 arcsec 90 per cent error for *Chandra* observations since we could not correct the bore sight for the *Chandra*-HRC observation). Using Gehrels (1986), this gives a 95 per cent confidence upper limit on the source count rate of 4×10^{-3} counts s^{-1}. Assuming the same spectral energy distribution as found from our *Chandra* ACIS-S observation and fixing $N_{\rm H}$ to 2.1×10^{21} cm^{-2}, the 95 per cent confidence

upper limit on the unabsorbed 0.5–10 keV source flux is 5.6×10^{-14} erg cm^{-2} s^{-1}, slightly higher than that derived by Wachter et al. (2005; in this we used *w3pimms*[2]). The upper limit on the flux derived from the *Chandra* HRC-I observation is consistent with the flux measured in our ACIS-S observation.

3 DISCUSSION

We have observed the field of the neutron star SXT 1M 1716−315 in X-rays with the *Chandra* satellite for ∼20 ks. We detect only one source in the *HEAO-1* error region. The spectrum of the source is soft with a 95 per cent upper limit to a power-law contribution of <19 per cent, making it unlikely that this source is a background AGN or an accreting white dwarf. The X-ray luminosity together with our stringent optical *I*-band and near-infrared K_s-band limits on the absolute magnitude rule out that the soft X-ray spectrum is due to coronal activity of a late-type star. Three other sources were found near the 90 per cent confidence *HEAO-1* error region. Even though the detected number of counts for these sources is too low to fit a spectrum, nearly all photons of all three sources are detected above 1.5 keV. Together with the fact that their positions do not agree with the *HEAO-1* error region, this makes them less likely candidates for the quiescent neutron star SXT.

We conclude that we have detected 1M 1716−315 in quiescence at a 0.5–10 keV source luminosity of 1.6×10^{32}–1.3×10^{33} erg s^{-1}. Fixing the value for the interstellar $N_{\rm H}$ to the value given in Christian & Swank (1997) [$(2.1 \pm 0.6) \times 10^{21}$ cm^{-2}], the resultant blackbody or NSA temperature is rather high for a neutron star SXT in quiescence, especially when taking into account that the source has been in quiescence for more than ≈16 yr (see below). We note that the $N_{\rm H}$ value given in table 12 of Christian & Swank (1997) depends on the spectral model that was used, both an absorbed blackbody plus thermal bremsstrahlung and Comptonization models give a $N_{\rm H}$ value of 4–5 $\times 10^{21}$ cm^{-2} (see tables 7 and 10 in Christian & Swank 1997). Indeed, when left as a free parameter in our X-ray spectral fits, the $N_{\rm H}$ is somewhat higher, although still consistent within 3σ with the value of $(2.1 \pm 0.6) \times 10^{21}$ cm^{-2}.

The *I*-band observations do not reveal an optical counterpart in the 99 per cent confidence 0.36 arcsec error circle down to a magnitude limit of $I > 23.5$. Using this limit and converting the $N_{\rm H}$ observed in outburst giving $A_I \sim 0.7$ (Schlegel, Finkbeiner & Davis 1998), taking $d = 5.1$–6.9 kpc (Jonker & Nelemans 2004), we derive that the absolute *I*-band magnitude $M_I \geqslant 8.6$–9.3. Equivalent calculations for the K_s band measurements result in $K_s \geqslant 5.1$–5.8. Hence, like 1H 1905+000 (Jonker et al. 2006), 1M 1716−315 is a candidate UCXB, although the secondary could also be an M dwarf. However, additional (circumstantial) evidence for an ultra-compact nature comes from the detected long (≈10 min) type I burst duration (Markert et al. 1976). Such long bursts can occur in sources accreting He at a low rate in UCXBs (see discussion in in't Zand, Jonker & Markwardt 2007) or sources accreting H-rich material at even lower rates (Peng, Brown & Truran 2007). Since the luminosity in outburst in the case of 1M 1716−315 was found to be above 10^{36} erg s^{-1}, the latter mode is less likely. The quiescent X-ray luminosity of 1M 1716−315 is higher than that of other (likely) UCXBs in quiescence (XTE J1751−305, XTE J0929−314, XTE J1807−294 and 1H 1905+000; Campana et al. 2005; Wijnands et al. 2005; Jonker et al. 2006). A plausible explanation for the higher quiescent luminosity is that the time-averaged mass accretion rate is higher in 1M 1716−315 than in the other UCXBs observed so far, possibly due to a shorter orbital period (Deloye & Bildsten 2003).

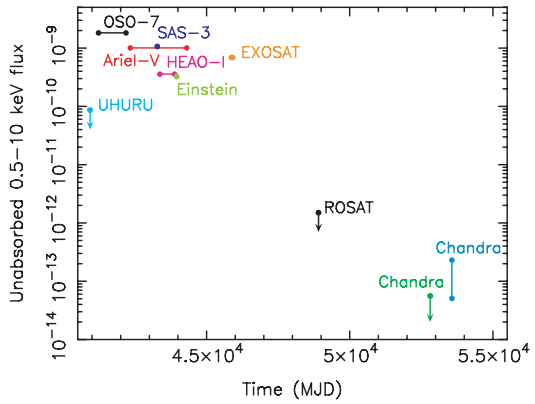

Figure 4. The unabsorbed 0.5–10 keV X-ray flux history of the source 1M 1716−315. The plotted ranges for each satellite indicate the time-span over which the source was detected on multiple occasions by that satellite. In order to convert fluxes given in the literature in other X-ray bands to the 0.5–10 keV band, we assume the spectrum to be well-represented by an absorbed power law with index 2 (except for the *ROSAT* and *Chandra* upper limit which were derived assuming a 0.3 keV blackbody). The absorption was taken to be 2.1×10^{21} cm^{-2} as found from spectra obtained in outburst by Einstein (Christian & Swank 1997). Arrows on the data points indicate upper limits to the X-ray flux.

We have plotted the long-term light curve of 1M 1716−315 in Fig. 4.[3] The most striking feature is the longevity of the outburst. The source has been active for nearly 13 yr before it returned to quiescence (Fig. 4). There is a time-span of 8.2 yr between the last detection by *EXOSAT* and the first non-detection by *ROSAT*. The source is likely to have returned to quiescence during this interval. There is 16.9 yr between the mid-point of this interval and the time of the *Chandra* observation that detected the source. Hence, the source has been in quiescence for 16.9 ± 4.1 yr. There is a growing number of quasi-persistent sources (the other sources being 2S 1711−339,[4] 4U 2129+47, KS 1731−260, MXB 1659−290, X 1732−304 and 1H 1905+000; Torres et al. 2004; Wijnands 2005; Cackett et al. 2006a,b; Jonker et al. 2006). Of these, only 1H 1905+000 has so far not been detected in quiescence. At present, there are three other quasi-persistent sources that are still in outburst, EXO 0748−676, GS 1826−238 and XTE J1759−220. In addition, HETE J1900.1−2455 has been in outburst for more than a year now. All these quasi-persistent sources have confirmed neutron star accretors, except XTE J1759−220 for which type I bursts or pulsations have not been reported so far.

ACKNOWLEDGMENTS

PGJ and SW acknowledge support from NASA grant GO4-5033X. PGJ and CGB acknowledge support from the Netherlands Organization for Scientific Research. We also acknowledge Frank Verbunt for

[2] Available at http://heasarc.gsfc.nasa.gov/Tools/w3pimms.html

[3] Data for Fig. 4 were taken or derived from Forman et al. (1978) (UHURU); Markert et al. (1975, 1976) and Markert et al. (1977) (OSO-7), Jernigan et al. (1978) (*SAS-3*), Reid et al. (1980) (*HEAO-1*), Christian & Swank (1997) (Einstein), Warwick et al. (1988) and Gottwald et al. (1995) (*EXOSAT*), Voges et al. (1999) (*ROSAT*) and this work.

[4] This source has had a ≳3 yr long outburst between MJD 50 739 and 51 751. On MJD 52 345, it was not detected with *Chandra* (see also Wilson et al. 2003).

useful discussions and the referee for useful comments that helped improve the manuscript.

REFERENCES

Arnaud K. A., 1996, ASP Conf. Ser. Vol. 101, Astronomical Data Analysis Software and Systems V. Astron. Soc. Pac., San Francisco, p. 17
Belczynski K., Taam R. E., 2004, ApJ, 603, 690
Brown E. F., Bildsten L., Rutledge R. E., 1998, ApJ, 504, L95
Cackett E. M., Wijnands R., Linares M., Miller J. M., Homan J., Lewin W. H. G., 2006a, MNRAS, 372, 479
Cackett E. M. et al., 2006b, MNRAS, 479
Campana S., Ferrari N., Stella L., Israel G. L., 2005, A&A, 434, L9
Chen W., Shrader C. R., Livio M., 1997, ApJ, 491, 312
Christian D. J., Swank J. H., 1997, ApJS, 109, 177
Colpi M., Geppert U., Page D., Possenti A., 2001, ApJ, 548, L175
Deloye C. J., Bildsten L., 2003, ApJ, 598, 1217
Forman W., Jones C., Cominsky L., Julien P., Murray S., Peters G., Tananbaum H., Giacconi R., 1978, ApJS, 38, 357
Gehrels N., 1986, ApJ, 303, 336
Gottwald M., Parmar A. N., Reynolds A. P., White N. E., Peacock A., Taylor B. G., 1995, A&AS, 109, 9
Güdel M., 2004, ARA&A, 12, 71
in't Zand J. J. M., Jonker P. G., Markwardt C. B., 2007, A&A, in press (astro-ph/0701810)
Jernigan J. G., Bradt H. V., Doxsey R. E., Dower R. G., McClintock J. E., Apparao K. M. V., 1978, Nat, 272, 701
Jonker P. G., Nelemans G., 2004, MNRAS, 354, 355
Jonker P. G., Galloway D. K., McClintock J. E., Buxton M., Garcia M., Murray S., 2004, MNRAS, 354, 666
Jonker P. G., Bassa C. G., Nelemans G., Juett A. M., Brown E. F., Chakrabarty D., 2006, MNRAS, 395
Makishima K. et al., 1981, ApJ, 244, L79
Markert T. H., Bradt H. V., Clark G. W., Lewin W. H. G., Li F. K., Schnopper H. W., Sprott G. F., Wargo G. F., 1975, IAU Circ, 2765, 1
Markert T. H., Backman D. E., McClintock J. E., 1976, ApJ, 208, L115
Markert T. H., Canizares C. R., Clark G. W., Hearn D. R., Li F. K., Sprott G. F., Winkler P. F., 1977, ApJ, 218, 801
Pavlov G. G., Shibanov I. A., Zavlin V. E., 1991, MNRAS, 253, 193
Peng F., Brown E. F., Truran J. W., 2007, ApJ, 654, 1022
Reid C. A., Johnston M. D., Bradt H. V., Doxsey R. E., Griffiths R. E., Schwartz D. A., 1980, AJ, 85, 1062
Rutledge R. E., Bildsten L., Brown E. F., Pavlov G. G., Zavlin V. E., Ushomirsky G., 2002, ApJ, 580, 413
Schlegel D. J., Finkbeiner D. P., Davis M., 1998, ApJ, 500, 525
Tawara Y., Hirano T., Kii T., Matsuoka M., Murakami T., 1984a, PASJ, 36, 861
Tawara Y. et al., 1984b, ApJ, 276, L41
Torres M. A. P., McClintock J. E., Garcia M. R., Murray S. S., 2004, Astron. Telegram, 233, 1
Verbunt F., van den Heuvel E., 1995, in Lewin W. H. G., van Paradijs J., van den Heuvel E. P. J., eds, X-ray Binaries. Cambridge Univ. Press, Cambridge, p. 457
Voges W. et al., 1999, A&A, 349, 389
Wachter S., Wellhouse J. W., Bandyopadhyay R. M., 2005, in Burderi L., Antonelli L. A., D'Antona F., di Salvo T., Israel G. L., Piersanti L., Tornambè A., Straniero O., eds, AIP Conf. Proc. 797: Interacting Binaries: Accretion, Evolution, and Outcomes. Springer, New York, p. 639
Warwick R. S., Norton A. J., Turner M. J. L., Watson M. G., Willingale R., 1988, MNRAS, 232, 551
Wijnands R., 2005, in Wass A. P., ed., Progress in Neutron Star Research. Nova Science Publishers, Hauppauge NY
Wijnands R., Miller J. M., Markwardt C., Lewin W. H. G., van der Klis M., 2001, ApJ, 560, L159
Wijnands R., Homan J., Heinke C. O., Miller J. M., Lewin W. H. G., 2005, ApJ, 619, 492
Wilson C. A., Patel S. K., Kouveliotou C., Jonker P. G., van der Klis M., Lewin W. H. G., Belloni T., Méndez M., 2003, ApJ, 596, 1220
Zacharias N., Urban S. E., Zacharias M. I., Wycoff G. L., Hall D. M., Monet D. G., Rafferty T. J., 2004, AJ, 127, 3043
Zavlin V. E., Pavlov G. G., Shibanov Y. A., 1996, A&A, 315, 141

This paper has been typeset from a TEX/LATEX file prepared by the author.